Case Studies in Thermal Engineering 15 (2019) 100535

Contents lists available at ScienceDirect

Case Studies in Thermal Engineering

journal homepage: http://www.elsevier.com/locate/csite

CFD optimization of return air ratio and use of upper room UVGI in combined HVAC and heat recovery system

Mohamad Kanaan

Beirut Arab University, Faculty of Engineering, Mechanical Engineering Department, P.O. Box 11-5020, Riad El Solh, Beirut, 1107-2809, Lebanon

A B S T R A C T

Several strategies and techniques have been recently developed to decrease energy consumption in heating, ventilation, and air-conditioning (HVAC) systems. One method is to recirculate a fraction of return air and make use of the remaining part (exhaust) to preheat fresh air in order to reduce the heating load. However, limitations must be imposed to the return fraction to maintain acceptable indoor air quality (IAQ).

The aim of this paper is to develop a computational fluid dynamics (CFD) model to predict the dispersion of CO_2 and airborne bacteria in all-air HVAC systems with aforementioned heat recovery system for known return air ratios as well as the disinfection of indoor air by upper room Ultraviolet Germicidal Irradiation (UVGI).

The developed model can be put to practical use for estimating the maximum allowable return that minimizes energy cost of the integrated system while maintaining acceptable IAQ. It can also be used to predict the minimum required UV output to eliminate any excess in bacteria count in the breathing zone without the need for additional fresh air intake at the supply.

1. Introduction

Energy utilized in heating, ventilation, and air conditioning (HVAC) represents up to 62% of the total energy consumption in the residential sector and up to 52% in offices [1]. Therefore, researchers have proposed and investigated different strategies and techniques that help save energy on HVAC systems. A common and practical method is the use of return air that almost has the temperature of the conditioned space. When a fraction of the exhaust air is mixed with fresh air in the upstream of the coil, the enthalpy between the air that flows over the coil and the supply air is reduced then the heating/cooling coil load and required energy input will be lower as compared to the 100% fresh air system. However, recirculating the return air will cause the air pollutants to build up in the indoor space and reach high concentration levels resulting in unacceptable indoor air quality (IAQ). Carbon dioxide (CO_2) level has been widely used as a surrogate indicator of IAQ and it is strongly related to odor perception. It is recommended that the indoor CO_2 concentration be within 700–1,000 ppm so that the comfort (odor) criterion is satisfied [2].

Another IAQ requirement that often may be more stringent is to maintain the airborne bacteria concentration within the standard limits in order to reduce the risk of cross infection in indoor environments [3]. The world health organization (WHO, 1988) recommended that the bacteria concentration in the breathing zone not to exceed 500 CFU/m^3 in offices and 200 CFU/m^3 in hospitals [4]. In HVAC return air systems, microbial contamination may become severe and disease transmission is more likely to occur. It is then quite important to use economically viable technologies that help decrease microbiological concentrations without the need for supplemental ventilation. One prominent solution is the use of upper room ultraviolet germicidal irradiation (UVGI), which is an effective and energy-efficient method for indoor air disinfection [5,6]. It was proven that UV light, when emitted at 254-nm wavelength, is able to inactivate germs by damaging their DNA. In practice, upper room UVGI devices are mounted on walls a minimum of 2 m high to ensure safe UV irradiance levels in the occupied zone [7,8]. The maximum allowable irradiance in the occupied zone is 0.002 W/m^2 for

E-mail address: m.kanaan@bau.edu.lb.

https://doi.org/10.1016/j.csite.2019.100535
Received 12 February 2019; Received in revised form 20 February 2019; Accepted 19 September 2019
Available online 22 September 2019

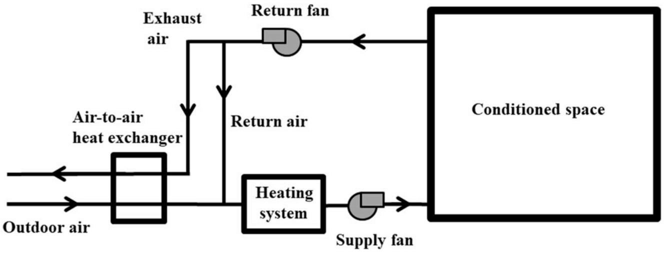

Fig. 1. Schematic of the return air HVAC heat recovery system [18].

8 h of exposure in order to prevent any skin or eye injury [9]. The success key for this technique is to have air interaction between the upper irradiated zone and the lower occupied zone so that the airborne pathogens are sufficiently exposed to UV light and then get inactivated [10,11].

The performance of any UV device in inactivating a particular microorganism is expressed by the fraction of microorganisms surviving following irradiation, given by:

$$C(t) = C_0 e^{-ZE_p t} \tag{1}$$

where C_0 is the initial microorganism concentration (CFU/m^3), Z is the microorganism's susceptibility to UV (m^2/J), E_p is the UV irradiance intensity (W/m^2), and $C(t)$ is the concentration at time t.

In spite of the fact that the use of return air has positive impact on energy performance of HVAC systems, it is constrained by IAQ requirements and then a compromise should be always made between energy efficiency and good IAQ. In other words, the return air ratio is dictated by the standard limits of the concentrations of air contaminants [3,12,13].

Another approach used for HVAC energy saving is heat recovery that aims to improve the energy efficiency of HVAC systems by utilizing the waste heat they release, such as transferring heat between exhaust air and fresh air. The demand of such applications has gradually increased due to the depletion of fossil fuel and different environmental impact issues including global warming [14,15]. Zhang et al. [16] investigated the performance of an exhaust air total heat recovery unit in a typical public building. He reported that the total cooling load of the whole building was reduced by more than 45%, while more than 20% reduction was reported for the heating load. Ramadan et al. [17] proposed a hybrid energy recovery system for all-air HVAC systems that allows recovering heat from the condenser, making use of the lost energy of exhaust air, and generating electricity using a thermoelectric generator. They showed that for a space cooling load of 100 kW, an electric power of 90 W can be generated per each 40×40 cm^2 flat plate.

This paper revisits the HVAC heat recovery system proposed and tested by Khaled and Ramadan [18]. The concept of this recovery system is to heat up the fresh outdoor air using relatively hot exhaust air in a traditional return air HVAC system during the heating season. Return air is mixed with fresh air (direct contact) and heat is recovered from the exhaust airflow and used to heat up the fresh air in an air-to-air heat exchanger (indirect contact) as shown in Fig. 1.

The authors studied the effect of hot air mass flow rate through the heat exchanger on the heat rate gained by the cold outdoor air and consequently on the heating load and power consumption. They reported power savings over 1 kW was a room with a heating load of approximately 4 kW when 20% of the exhaust airflow was used for heat recovery. Nevertheless, it is well known that heat transfer between the outdoor (cold) air stream and the exhaust (hot) air stream is more effective in mixing as the two fluids are in direct contact. Therefore, increasing the return air ratio at the expense of the fraction of exhaust flow used for heat recovery in the heat exchanger will result in better energy efficiency for the system. However, the amount of re-circulated return air is restricted by IAQ requirements as explained earlier on. The aim of the current study is to optimize, using computational fluid dynamics (CFD) modeling, the choice of the return air ratio in the HVAC heat recovery system and the integration of upper room UVGI in order to maintain good and healthy IAQ at minimum energy cost.

2. Methods

A typical office space containing two workstations one for a healthy occupant and the other for an infected occupant is chosen as a case study. A detailed steady-state three-dimensional CFD model is developed to predict the airflow patterns, thermal fields, species transport as well as the UV inactivation of germs using ANSYS Fluent, which is one of the most powerful nonlinear finite volume analysis software in the world [19]. Many reviews concluded that CFD applications to indoor airflow simulation have achieved considerable successes [20–26]. Li and Nielsen [27] reported that CFD can give reasonably accurate predictions when correct governing equations and boundary conditions, and appropriate numerical algorithms are carefully selected. The indoor air quality is determined based on both CO_2 and bacteria concentrations in the breathing zone. In the present study a parametric study will be performed where the return air ratio will be varied in order to determine the maximal value that maintains no more 700 ppm CO_2 concentration in the breathing air layer for seated occupants [2,3]. Additional simulation runs will be conducted to determine the minimum required UV output to keep the bacteria concentration in the breathing layer at the standard limit of 500 CFU/m^3 without bringing in additional fresh air to the conditioned space. An energy analysis will be then presented to evaluate the energy performance of the integrated system.

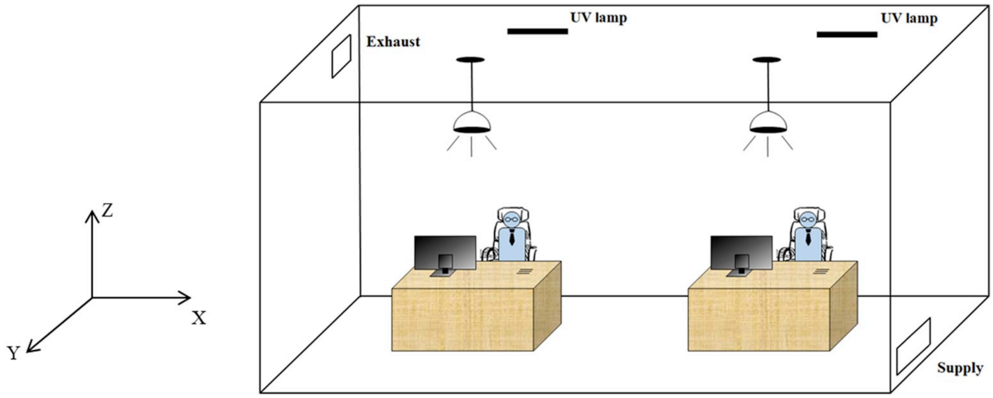

Fig. 2. Schematic of the simulated office space.

2.1. System description

The study considers a 6 m (L) × 4 m (W) × 2.8 m (H) office space located in Beirut and having two external walls and two partitions. The room contains two workstations each equipped with a desk, a chair, and a computer as shown in Fig. 2. The room has a heating load of 2.5 kW with a sensible heat ratio of 0.8 and it is conditioned by a conventional mixing ventilation system integrated with the heat recovery system presented in Ref. [18] to heat the fresh air using exhaust air. The air-to-air heat exchanger in use is assumed to have an average effectiveness of 0.8. The indoor design conditions are: dry-bulb temperature of 22 °C and relative humidity of 50%, whereas the outdoor design conditions are dry-bulb temperature of 7 °C and web-bulb temperature of 4 °C (January). Air is supplied to the space at a temperature of 45 °C and a rate of 0.11 kg/s. The supply and exhaust grills have areas of 80 × 20 cm^2 and 40 × 20 cm^2 respectively. Each occupant emits 0.31 L/min CO_2 [28,29], and the infected occupant emits 700 CFU/min of *Staphylococcus aureus* [6], which is common type of contagious airborne bacteria [30].

2.2. CFD methods

The CFD model is meant to capture the behavior of the mixed air inside the indoor space and its interactions with thermal plumes from the heat sources, the turbulence effects, the transport of species, and the germicidal effect of UV light. For simplicity and in order to reduce the mesh size, an occupant was represented by a cylinder of diameter of 0.47 m and height of 1.1 m (seated) [31,32] with constant heat flux of 42.8 W/m^2. The occupant's mouth was simulated by a circular hole of area 1.2 cm^2 [33] and an average exhalation rate of 8.4 L/min was assumed for breathing and talking [34]. The room geometry was discretized into 962,303 tetrahedral elements ensuring grid independence of the solution with refinement around the boundaries and species sources. The mesh quality was ensured with maximal skewness less than 0.9. The breathing layer is defined as being the horizontal air region between z = 0.88 m and z = 1.22 m in the computational domain. The governing equations were discretized using the second order upwind scheme. However, the pressure term was discretized using the first order STANDARD. The SIMPLE algorithm was used for pressure-velocity coupling. The solution was considered convergent when the scales residuals reached 5×10^{-5}, the net heat and mass fluxes became less than 5% of the smallest flux in the computational domain, and the species concentrations in the breathing zone were stabilized.

2.2.1. Airflow and thermal modeling

The airflow was simulated using the standard k–ε turbulence model that is known to produce accurate and experimentally validated results for indoor ventilation problems [35–37]. Buoyancy was modeled using the Boussinesq approximation. Radiation was accounted for by activating the surface to surface (S2S) model which calculates the energy exchange in an enclosure of gray-diffuse surfaces. The energy reflected from a surface is computed using the absolute temperature, emissivity, and reflectivity of that surface and the energy flux incident on it from the surroundings. The radiation exchange between two surfaces depends on their size, separation distance, and orientation. These parameters are taken into account using view factors computed by the ANSYS solver.

2.2.2. Bacteria transport modeling

Viable germs are contained in aerosols expelled by infected people during expiratory activities. The majority of these germ-carrying particles evaporate within milliseconds to become droplet nuclei (<5 μm) and remains suspended in air for long periods of time [38]. Therefore, the passive scalar approach is reasonably used to determine the bacteria concentration fields in built environments since they are governed by the airflow patterns. The following equation for airborne bacteria transport is to be solved by the CFD solver [39]:

$$\nabla.(UC) + \nabla.[(D + D_t)\nabla C] - Z.I.C = 0 \tag{2}$$

where U is the air velocity, C is the bacteria concentration, D is the Brownian diffusivity, D_t is Eddy's diffusivity. The last term in Equation (2) is the sink term representing the UV inactivation of bacteria where Z is the bacteria susceptibility to UV (Z = 0.35 m^2/J for

Table 1
Boundary conditions used in the simulations.

Boundary	Type	Details
Supply	Velocity inlet	Velocity: 0.5 m/s, Turbulent intensity: 10%, Hydraulic diameter: 0.32 m, Temperature: 45 °C, Species molar fraction: $CO_2 = 0.0004$ and *S.aureus* = zero for the 100% fresh air case and UDF for recirculation.
Exhaust	Outflow	–
Occupant simulator (cylinder)	Wall – no slip	Heat flux: 42.8 W/m^2
Occupant mouth (cylinder hole)	Velocity inlet	Velocity: 1.2 m/s, Turbulent intensity: 10%, Hydraulic diameter: 0.01236 m, Temperature: 34 °C, CO_2 molar fraction: 0.036, *S.aureus* molar fraction (infected occupant): 7.15×10^{-11} ar
Computer	Wall – no slip	Heat output: 93 W
Ceiling	Wall – no slip	Heat flux: 12 W/m^2 (lighting)
Exposed walls	Wall – no slip	Heat flux: 45.9 W/m^2
Floor	Wall – no slip	Heat flux: 25.6 W/m^2

S. aureus [40]), and I is the UV irradiance intensity at the centroid of the cell.

2.2.3. UV modeling

The upper room UVGI system is needed to reduce the bacteria concentration when it exceeds the maximum allowable level in the breathing layer. The proposed system consists of two identical linear UV lamps that are installed and centered on two opposite walls at a height of 2.3 m. The irradiance distribution inside the office space is predicted using the experimentally validated model of Kowalski et al. [41]. This model is based on view factors, but it disregards the irradiation refection by the room surfaces assuming diffusive enclosure. The spatial UV irradiance is computed as follows:

$$I = \frac{E_{UV}}{2\pi rl} F_{d1-2} \tag{3}$$

where E_{UV} is the UV output of the lamp, r and l are the radius and length of the lamp respectively, and $F_{d1-2}$is the view factor from a differential surface to the lamp.

The UV model was incorporated into the CFD solver through a user-defined function (UDF) written in C++ to compute the UV fields and the associated sink terms for the transport equation applied to each cell in the computational grid. A similar CFD-UV model with same deployed models, boundary conditions, and discretization schemes was developed and experimentally validated in Ref. [42].

2.2.4. Boundary conditions

Appropriate selection of boundary conditions to be used in the simulations is quite important for obtaining accurate results. The supply grill was specified as velocity inlet while outflow condition was imposed to exhaust. The recirculation of return air is simulated using a UDF that computes the species concentration at the supply, in terms of return air ratio r, as follows:

$$C_{\mathrm{supply}} = (1 - r)C_{outdoor} + rC_{return} \tag{4}$$

All solid surfaces such as heated cylinders, room walls, equipment, and furniture were considered as walls (no-slip condition). The boundary conditions used in the parametric study are summarized in Table 1.

2.3. Parametric study and energy analysis

The purpose of the parametric study is to optimize the energy performance of the integrated heat recovery system while keeping acceptable and healthy air quality in the breathing layer. The concerned office was simulated using different values of return air ratio in order to determine the maximal allowable value that results in 700 ppm in the breathing layer. Since the bacteria concentration is usually more stringent than that of CO_2, an additional set of simulations is needed to determine the minimum required UV output so that the bacteria concentration drops to 500 CFU/m^3 in the breathing layer without the need for additional ventilation air. The energy analysis is then performed for each case and the energy savings achieved on the system comparing to 100% fresh air are also quantified. The heating coil capacity is given, in kW, by:

$$\dot{Q} = \dot{m}_a \left(h_{\mathrm{supply}} - h_{mix}\right) \tag{5}$$

where h_{mix} is the enthalpy of the air resulting from mixing the fresh outdoor air with return air in the upstream of the heating coil and is computed as follows:

$$h_{mix} = (1 - r)h_{o,downstream} + rh_{return} \tag{6}$$

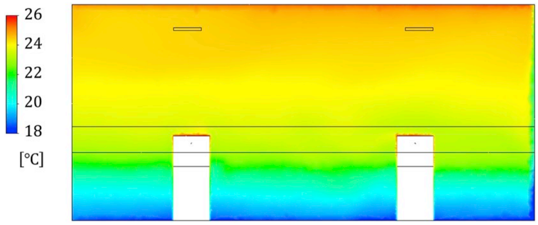

Fig. 3. Indoor temperature distribution at y = 3 m

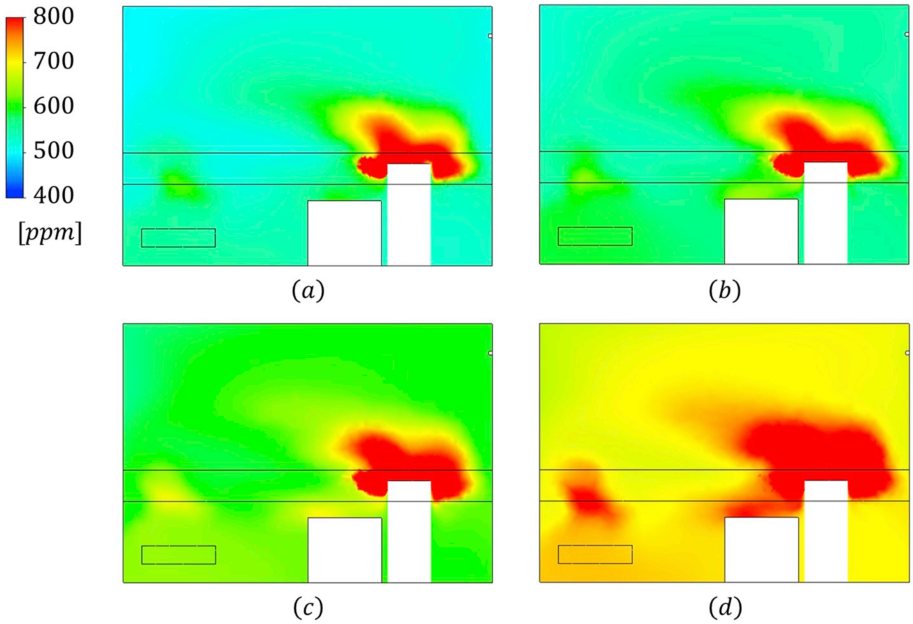

Fig. 4. CO_2 concentration contour plots at x = 4.45 m for (a) $r = 0$ (100% fresh air), (b) $r = 0.2$, (c) $r = 0.4$ and (d) $r = 0.6$.

Where $h_{o,downstream}$ is the enthalpy of the fresh air after passing through the heat exchanger. It is calculated using the effectiveness of the heat exchanger which is given, for balanced flows, by Ref. [43]:

$$\eta = \frac{h_{o,downstream} - h_{o,upstream}}{h_{exhaust} - h_{o,upstream}} \tag{7}$$

where $h_{o,upstream}$ is the fresh air enthalpy in the upstream of the heat exchanger.

3. Results and discussion

3.1. Thermal distribution

Since return air is mixed with outdoor air in the upstream of the heating coil, the supply air temperature remains unchanged in all cases. Consequently, the indoor temperature profiles are the same throughout all simulations and they are shown in Fig. 3 on cut plane y = 3 m. The warm supply air jet displaces upward, due to its relatively low density and momentum, leaving the zone near floor at relatively low temperature. It is noteworthy to mention that low temperature at the floor level may cause occupants' discomfort in their feet which calls for improvements on the ventilation openings design.

3.2. Optimal return air ratio

The office under study was simulated first for the 100% fresh air case and then for three mixing cases with different values of return air ratio ($r = 0.2$, $r = 0.4$ and $r = 0.6$). Fig. 4 shows the indoor CO_2 distribution on a cut plane passing through an occupant's mouth (x = 4.45 m). Since the airflow patterns are the same in all simulated cases, the species concentrations have similar profiles while values are increasing with the return air ratio.

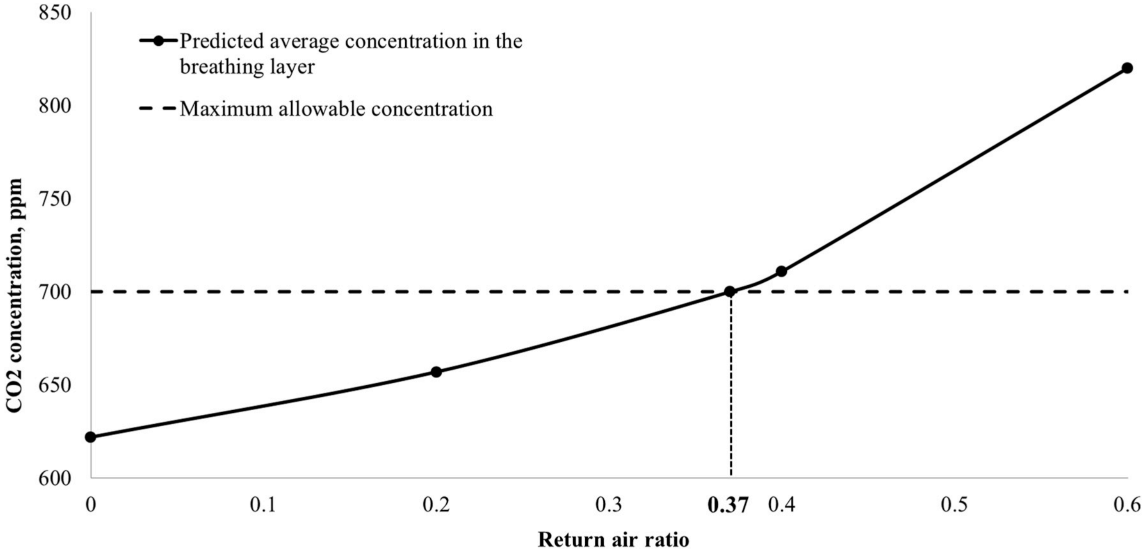

Fig. 5. Variations of average CO_2 concentration in the breathing layer with return air ratio.

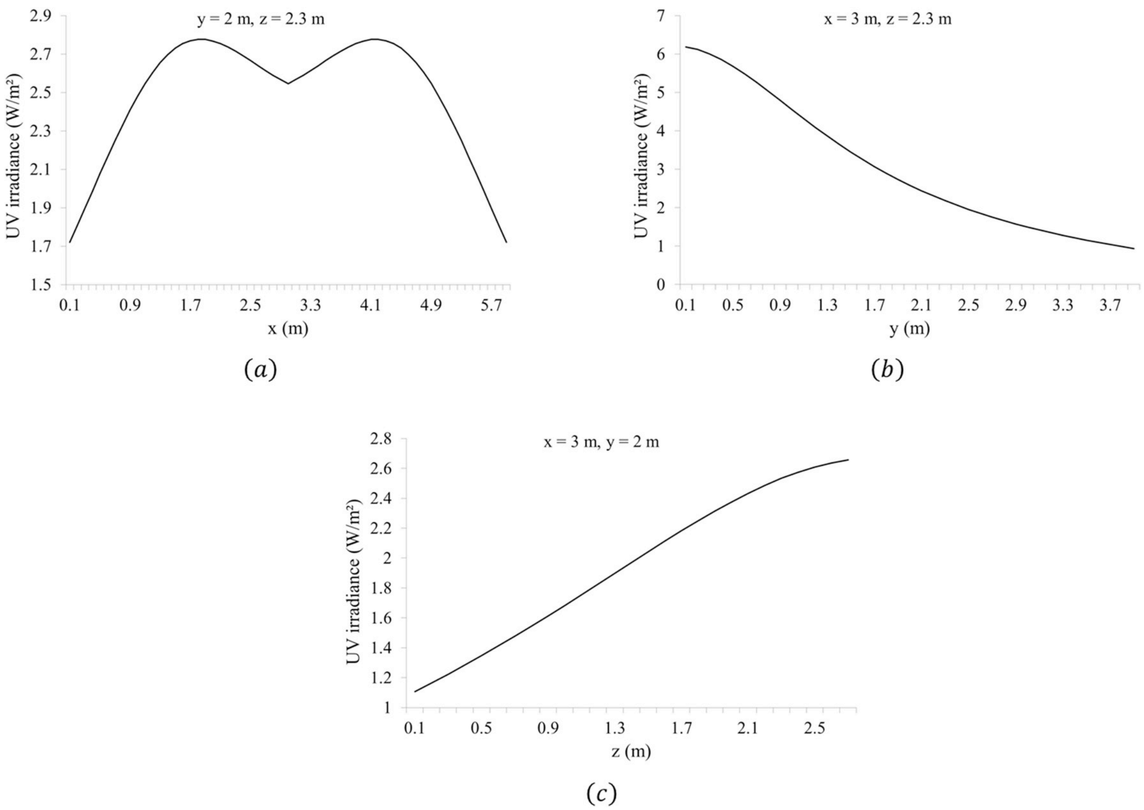

Fig. 6. UV irradiance distributions in (a) x-direction, (b) y-direction, and (c) z-direction.

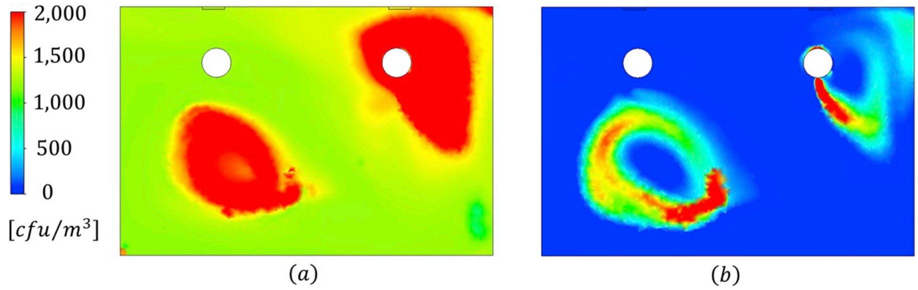

Fig. 7. Contour plots for *S. aureus* concentration at z = 1.05 m for the 37% return case (a) without UV and (b) with UV output of 18 W.

Table 2
Summary of enthalpies used in the energy analysis.

Outdoor design conditions 7 °C db 4 °C wb	$h_{o,fresh} = 18kJ/kg$	Indoor design conditions 22 °C db RH = 50%	$h_{return/exhaust} = 44kJ/kg$
Supply conditions 45 °C db at SHF = 0.8	$h_{supply} = 74.5kJ/kg$	Heat exchanger effectiveness: 0.9	$h_{o,downstream} = 41.4kJ/kg$

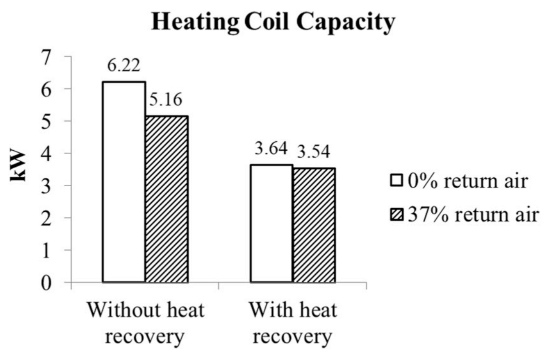

Fig. 8. Comparative graph for heating coil capacity.

The variations of the volume-averaged CO_2 concentration in the breathing layer with return air ratio along with the return air ratio resulting in 700 ppm in the breathing zone ($r = 0.37$) obtained by interpolation are shown in Fig. 5.

3.3. Minimum required UV output

Simulating the office space with $r = 0.37$ showed a predicted volume-average *S. aureus* concentration of 1,584 CFU/m^3 in the breathing layer that exceeds the WHO maximal allowable value of 500 CFU/m^3. The concentration value in CFU/m^3 is obtained by multiplying the molar fraction by the bacteria density and then dividing by the mass of one bacterium [6]. Several simulations were performed using the developed CFD-UV model for different UV outputs. Results showed that a UV output of (2 × 9 W) is required to obtain the standard limit of bacteria concentration by achieving a disinfection rate of 68.4% in the breathing layer. Fig. 6 shows the predicted distribution of UV irradiance in (a) x-direction at y = 2 m and z = 2.3 m, (b) y-direction at x = 3 m and z = 2.3 m, and (c) z-direction at x = 3 m and y = 2 m.

The bacteria distribution in the office at the height of z = 1.05 m with and without the use of UVGI is shown in Fig. 7 where effective air disinfection was achieved at the breathing level.

3.4. Energy savings

The use of upper room UVGI is more economical for decreasing indoor bacteria concentrations than increasing the fresh air intake at the supply. The rated power of the proposed UVGI system (18 W) is very small compared to the power consumption of the heating system and can be ignored. The enthalpies of airstreams involved in the analysis are obtained from design conditions and from Equations (6) and (7), and are summarized in Table 2.

The heating coil capacity for the 100% fresh air and for $r = 0.37$ with and without the heat recovery system are shown in Fig. 8. The use of return air at a ratio of 0.37 with the heat recovery system is present achieves less energy cost with savings of 43% on the heating system compared to the base case of 100% fresh air without heat recovery and maintains an acceptable and healthy IAQ while only

18 W of UV is required.

4. Conclusion

A steady-state CFD model is developed to predict indoor CO_2 and bacteria transport in mixing ventilation systems. Also, the CFD model is integrated with a mathematical UV irradiance model to simulate the upper UVGI disinfection of indoor airborne bacteria. The CFD-UV model is then used to optimize the operation of a published HVAC heat recovery system in a typical office space containing an infected case. In this system, outdoor air is preheated using exhaust air before mixing with a fraction of return air in the upstream of the heating coil. The target of the present optimization exercise is to minimize energy cost while maintaining good IAQ and reducing the risk of airborne cross infection in the office. Several simulations were performed while changing the return air ratio and results showed that the latter can reach 37% without violating the ASHRAE standard for CO_2 concentration in the breathing layer. However, UV output of 18 W is still needed to satisfy the WHO recommendation for maximal allowable bacteria concentration. In this case, 43% of energy savings was achieved on the heating system when comparing with the base case of 100% fresh air with no heat recovery, and IAQ is maintained acceptable in the breathing layer.

Conflicts of interest

There is no conflicts interest.

References

[1] L. Perez-Lombard, J. Ortiz, C. Pout, A review on buildings energy consumptions, J. Energy Build. 40 (3) (2008) 294–298.
[2] ASHRAE, Standard 62-2007. Ventilation for Acceptable Indoor Air Quality, American Society of Heating. Refrigeration and Air Conditioning Engineers, Inc., Atlanta, GA, 2007.
[3] M. Kanaan, N. Ghaddar, K. Ghali, Localized air-conditioning with upper-room UVGI to reduce airborne bacteria cross-infection, in: Building Simulation, vol 9, Tsinghua University Press, 2016, pp. 63–74. No. 1.
[4] WHO, Indoor Air Quality: Biological Contaminants. World Health Organization, European Series, 1988 n. 31, Copenhagen, Denmark.
[5] S.L. Miller, J.M. Macher, Evaluation of a methodology for quantifying the effect of room air ultraviolet germicidal irradiation on airborne bacteria, Aerosol Sci. Technol. 33 (3) (2000) 274–295.
[6] M. Kanaan, N. Ghaddar, K. Ghali, G. Araj, New airborne pathogen transport model for upper-room UVGI spaces conditioned by chilled ceiling and mixed displacement ventilation: enhancing air quality and energy performance, Energy Convers. Manag. 85 (2014) 50–61.
[7] E.A. Nardell, S.J. Bucher, P.W. Brickner, C. Wang, R.L. Vincent, K.,. Becan-McBride, J.D. Wright, Safety of upper-room ultraviolet germicidal air disinfection for room occupants: results from the Tuberculosis Ultraviolet Shelter Study, Public Health Rep. 123 (1) (2008) 52–60.
[8] P. Xu, J. Peccia, P. Fabian, J.W. Martyny, K.P. Fennelly, M. Hernandez, S.L. Miller, Efficacy of ultraviolet germicidal irradiation of upper-room air in inactivating airborne bacterial spores and mycobacteria in full-scale studies, Atmos. Environ. 37 (3) (2003) 405–419.
[9] American Conference of Governmental Industrial Hygienists, TLVs and BEIs, ACGIH, Cincinnati, 1999.
[10] M. First, S.N. Rudnick, K.F. Banahan, R.L. Vincent, P.W. Brickner, Fundamental factors affecting upper-room ultraviolet germicidal irradiation—part I. Experimental, J. Occup. Environ. Hyg. 4 (5) (2007) 321–331.
[11] S. Zhu, J. Srebric, S.N. Rudnick, R.L. Vincent, E.A. Nardell, Numerical modeling of indoor environment with a ceiling fan and an upper-room ultraviolet germicidal irradiation system, Build. Environ. 72 (2014) 116–124.
[12] V. Vakiloroaya, B. Samali, A. Fakhar, K. Pishghadam, A review of different strategies for HVAC energy saving, Energy Convers. Manag. 77 (2014) 738–754.
[13] M. Kanaan, N. Ghaddar, K. Ghali, Simplified model of contaminant dispersion in rooms conditioned by chilled-ceiling displacement ventilation system, HVAC R Res. 16 (6) (2010) 765–783.
[14] M. Ramadan, M.G. El Rab, M. Khaled, Parametric analysis of air–water heat recovery concept applied to HVAC systems: effect of mass flow rates, Case Stud. Ther. Eng. 6 (2015) 61–68.
[15] N.S. Ekaab, N.H. Hamza, M.T. Chaichan, Performance and emitted pollutants assessment of diesel engine fuelled with Biokerosene, Case Stud. Ther. Eng. (2018) 100381.
[16] X. Zhang, A study of the impact of exhaust heat recovery on public building energy consumption in seasonal extreme temperatures, Int. J. Simul. Syst. Sci. Technol. 17 (48) (2016).
[17] M. Ramadan, S. Ali, H. Bazzi, M. Khaled, New hybrid system combining TEG, condenser hot air and exhaust airflow of all-air HVAC systems, Case Stud. Ther. Eng. 10 (2017) 154–160.
[18] M. Khaled, M. Ramadan, Heating fresh air by hot exhaust air of HVAC systems, Case Stud. Ther. Eng. 8 (2016) 398–402.
[19] Y.F. Guan, F. GAO, W.B. ZHAO, J. YU, Secondary development of modified Cambridge model in ANSYS software, Rock Soil Mech. 3 (2010) 058.
[20] G.E. Whittle, Computation of air movement and convective heat transfer within buildings, Int. J. Ambient Energy 7 (3) (1986) 151–164.
[21] Q. Chen, Significant questions in predicting room air motion, ASHRAE Transact. 98 (1) (1992) 929–939.
[22] S.J. Emmerich, S.J. Emmerich, Use of Computational Fluid Dynamics to Analyze Indoor Air Quality Issues, National Institute of Standards and Technology, 1997.
[23] J.D. Spengler, Q. Chen, Indoor air quality factors in designing a healthy building, Annu. Rev. Energy Environ. 25 (1) (2000) 567–600.
[24] Z. Zhai, Application of computational fluid dynamics in building design: aspects and trends, Indoor Built Environ. 15 (4) (2006) 305–313.
[25] A.A. Hussain, B. Freegah, B.S. Khalaf, H. Towsyfyan, Numerical investigation of heat transfer enhancement in plate-fin heat sinks: effect of flow direction and fillet profilet, Case Stud. Ther. Eng. (2019) 100388.
[26] Y. Zhou, Y.L. Cheng, N. Zhang, H.B. Shi, Numerical simulation study of novel air-cooled condenser with lateral air supply, Case Stud. Ther. Eng. 13 (2019) 100354.
[27] Y. Li, P.V. Nielsen, CFD and ventilation research, Indoor Air 21 (6) (2011) 442–453.
[28] D.S. Dougan, L. Damiano, CO2-based demand control ventilation: do risks outweigh potential rewards? ASHRAE J. 46 (10) (2004) 47.
[29] A. Persily, J. Gorfain, Analysis of Ventilation Data from the US Environmental Protection Agency Building Assessment Survey and Evaluation (BASE) Study, Report of National Institute of Standards and Technology, NISTIR, 2008, p. 7145.
[30] M.R. Vriens, A.C. Fluit, A. Troelstra, J. Verhoef, C. van der Werken, Is methicillin-resistant Staphylococcus aureus more contagious than methicillin-susceptible S. aureus in a surgical intensive care unit? Infect. Control Hosp. Epidemiol. 23 (9) (2002) 491–494.
[31] F. Causone, S.P. Corgnati, M. Filippi, B.W. Olesen, Experimental evaluation of heat transfer coefficients between radiant ceiling and room, Energy Build. 41 (6) (2009) 622–628.
[32] M. Alain, G. Kamel, G. Nesreen, A simplified combined displacement and personalized ventilation model, HVAC R Res. 18 (4) (2012) 737–749.
[33] J. Gupta, C. Lin, Q. Chen, Characterizing exhaled airflow from breathing and talking, Indoor Air 20 (2010) 31–39.

[34] C. Habchi, K. Ghali, N. Ghaddar, W. Chakroun, S. Alotaibi, Ceiling personalized ventilation combined with desk fans for reduced direct and indirect cross-contamination and efficient use of office space, Energy Convers. Manag. 111 (2016) 158–173.
[35] C.G. Speziale, On nonlinear kl and k-ε models of turbulence, J. Fluid Mech. 178 (1987) 459–475.
[36] A.J. Gadgil, C. Lobscheid, M.O. Abadie, E.U. Finlayson, Indoor pollutant mixing time in an isothermal closed room: an investigation using CFD, Atmos. Environ. 37 (39–40) (2003) 5577–5586.
[37] M.P. Wan, C.Y. Chao, Numerical and experimental study of velocity and temperature characteristics in a ventilated enclosure with underfloor ventilation systems, Indoor Air 15 (5) (2005) 342–355.
[38] L. Morawska, Droplet fate in indoor environments, or can we prevent the spread of infection? Indoor Air 16 (2006) 335–347.
[39] E.A. Hathway, C.J. Noakes, P.A. Sleigh, L.A. Fletcher, CFD simulation of airborne pathogen transport due to human activities, Build. Environ. 46 (12) (2011) 2500–2511.
[40] D.G. Sharp, The effects of ultraviolet light on bacteria suspended in air, J. Bacteriol. 39 (5) (1940) 535.
[41] W. Kowalski, W.P. Bahnfleth, D.L. Witham, B.F. Severin, T.S. Whittam, Mathematical modeling of ultraviolet germicidal irradiation for air disinfection, Quant. Microbiol. 2 (3) (2000) 249–270.
[42] M. Kanaan, N. Ghaddar, K. Ghali, G. Araj, Upper room UVGI effectiveness with dispersed pathogens at different droplet sizes in spaces conditioned by chilled ceiling and mixed displacement ventilation system, Build. Environ. 87 (2015) 117–128.
[43] M.K. Drost, Air-to-air heat exchanger performance, Energy Build. 19 (3) (1993) 215–220.